Design of a New Type of XBT Profiler by the CAE Technique

Kotarou TETSUMURA*, Nariyuki MOHNAI*, Yasuzumi Fujimori**

and Nobuo Kimura**

* SEC Co., Ltd, Hokkaido, Japan

** Faculty of Fisheries Sciences, Hokkaido University, Japan

Abstract

The XBT (Expendable Bathythermograph) is variously used in broad areas of oceanographic observation at the moment. It is required to develop a new type frame corresponding to various needs for measuring information. In this study, it is confirmed that the numerical simulation based on the fluid dynamics technique is effective for designing the optimal frame of a new type of multi-functional XBT profiler.

1 Background

On the oceanographic observation for a vertical distribution of water temperature and salinity, CTD (Conductivity Temperature Depth profiler) is generally used. However, it is difficult to measure the wide area for a short time, since the measurement with CTD is done under the stationary state of ship lying to and the measurement time is influenced by the targeted water depth. Then, the expendable type sensors such as XBT and XCTD are used to efficiently observe a wide area. Recently, according to the increasing needs for the marine resource investigation like the methane hydrate on the seabed, the development of the multi-functional types XBT which can collect the image data, etc. has been proceeding. On the essential factor for

such profiler's frame, it is required that the sinking speed is adequate for the measurement without a spin. Therefore, the new frame design including not only the smoothly shape to reduce the flow-resistance in fluid but also proper current for the probes of sensor without damage becomes necessary.

In this paper, we focus attention on the development of a new type of XBT profiler based on the CAE (computer aided engineering) technique and the effectiveness for the designing is confirmed by the numerical simulations [1].

2 The frame design of the XBT profiler

Firstly, the conditions of plan of the new type of XBT profiler are decided as follows:

1. The tip of the body is flat with 29.0 mm diameter for installing a CCD camera and LED lights and the maximum diameter of the frame is 75.0 mm.
2. The length of the body is ranged from 200.0 mm to 300.0 mm which is enough size to install a various measuring instrument.
3. A couple of fins are added to prevent twisting signal line and to take a stable moving picture with the CCD camera.
4. Twin channels along the frame are set out to avoid protruding of the probe of sensor on the frame surface. Current distribution in the channels should be proper for the measurement.

The conceptual structure based on the above conditions without the fins is shown in Fig. 1. Note that the body will be constructed from the dissolved materials for the seawater made from shell of scallop, considering for the effect for the environment after measurement.

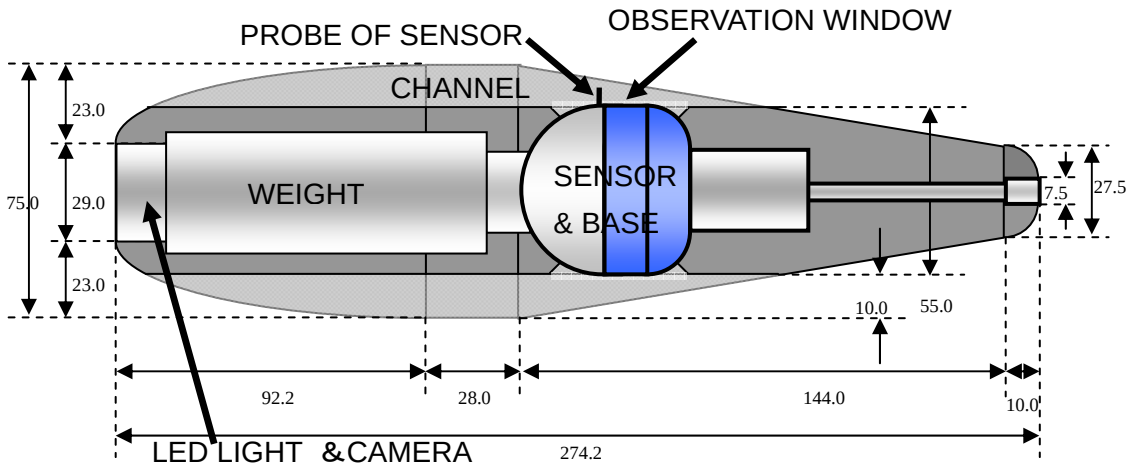

Fig. 1 Concept of structure design without fins

3 Method

Used by the 2D numerical simulation, we made the prototype of the body optimized the current distribution around the frame. The design and overview of the model are shown in Fig. 2. Improving the design of the body on the 3D simulations, twelve types of bodies were newly designed. As for the design of the fins, six types which were different shapes and installation positions were designed. Numerical simulations were conducted for all of the combinations of bodies and fins. Then, the one meeting the requirement was selected as a new type of XBT profiler among them. As for the configuration and location of the fins, four approximately rectangular fines (height 33mm×width 20mm) which were set at 0.2m distance from the tail at angle with 45.0 degrees for the channels were adopted.

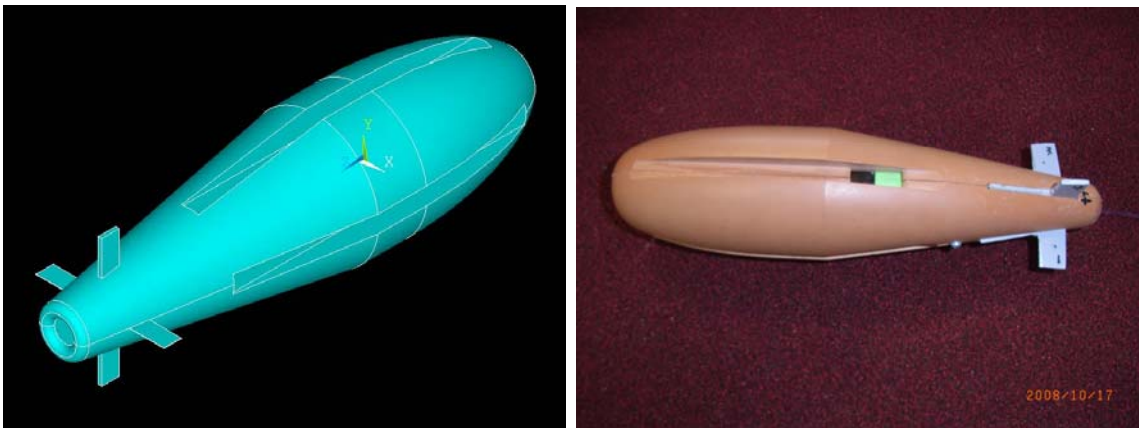

Fig. 2 The design and photograph of the prototype optimized by the 2D numerical simulation

4 Analysis

For the numerical analyses, we used the ANSYS ICEM CFX and Design Modeler made by the Cybernet Inc. [2-3]. Numerical analysis technique is fundamentally based on the finite element method (FEM) applying for fluid dynamics [4].

Utilized numerical analyzing method is the finite element method (FEM). Simple idea of 3D elements and nodes is shown in Fig. 3. Details related to the fundamental equation of fluid substance and their formulations are shown in Appendix 1-2.

Computational area is solidness in length of 1.500 m a side around the profiler model. Utilized mesh is tetrahedral mesh automatically constructed and the node number

under the simulation is about 150,000. Boundary condition for the simulation is shown in Table 1. The mean current velocities on the inlet are the uniform flow with $\bar{\boldsymbol{u}} = 4.0$ m/s in the x-direction, $\bar{\boldsymbol{v}} = \bar{\boldsymbol{w}} = 0.0$ m/s in the y and z-directions. The mean current velocities on the right, left, upper and lower side are also $\bar{\boldsymbol{u}} = 4.0$ m/s, and $\bar{\boldsymbol{v}} = \bar{\boldsymbol{w}} = 0.0$ m/s in the condition of traction free. The mean current velocities on the profiler surface are $\bar{\boldsymbol{u}} = \bar{\boldsymbol{v}} = \bar{\boldsymbol{w}} = 0.0$ m/s in the condition of no slip. The standard value of the pressure on the outlet is 0.0 Pa in the condition of traction free.

On the computational condition, water density is 998.2kg・m^{-3}, viscosity is 1.0×10^{-3}Pa・s, conductivity is 0.6eW/(m・K), and specific heat is $4.182e^{3}$J/(kg・K). The turbulent flow model is used in the SST (Sheer Stress Transport) model [5].

Motion equation of the profiler in the vertical direction was applied for the 1st dimensional motion equation based on the tank test and estimated the downwelling velocity of the profiler. Detail related to the motion equation is shown in Appendix 3. Fundamental physical values used for the estimation are follows: mass m: 1.260kg, volume V: 0.758×10^{-3} m^3, projected area A: 4.098×10^{-3} m^2, density ρ : 9782.36 kg・m^{-2}・s^{-2} , Reynolds number Re: 1.089×10^{6} with the water temperature $20.0^{\circ}C$. The drag coefficient C_D is 0.0378 estimated by the tank test on the condition that the attacking angle is zero.

Table1 Boundary condition for the simulation

position	mean current	traction
inlet	$\bar{u} = 4.0,\quad \bar{v} = \bar{w} = 0.0$	-
outlet	$\bar{u} = 4.0,\quad \bar{v} = \bar{w} = 0.0$	free
right and left side	opening	free
upper and lower side	opening	free
surface on the profiler	$\bar{u} = \bar{v} = \bar{w} = 0.0$	no slip

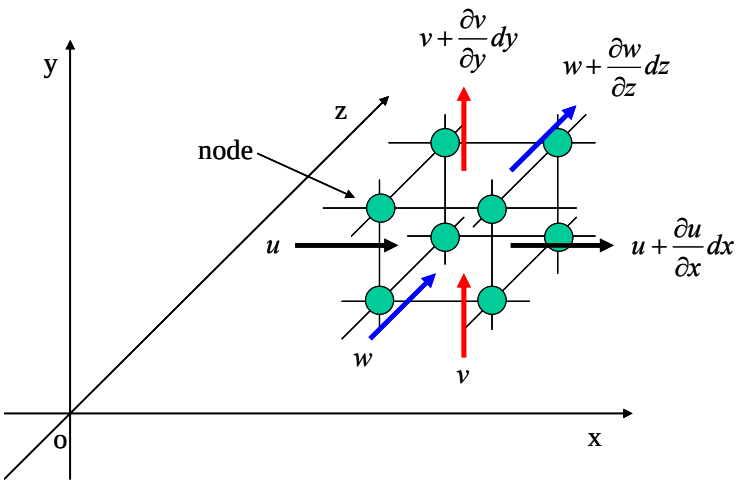

Fig. 3 Idea of Finite Element Method (FEM)

5 Results

Simulated pressure distribution around the XBT profiler in the 4.0m/s is shown in Fig. 4, and the pressure distributions in front and back are also shown in Fig. 5 (a)-(b). Current velocity distribution around the XBT profiler is shown in Fig. 6. Streamline around the channel along the body is shown in Fig. 7.

As shown in Fig. 4 and Fig. 5 (a)-(b), the pressure on the whole body is small except for the great pressure in front due to the flat shape. Further, the pressure in the tail is not big. It means that the current of on the surface of the XBT profiler smoothly streams without the separation from the frame. As shown in Fig. 6 and Fig. 7, the current velocity for fins is sufficient with over 2.0m/s since the fines are set at away from the tail on which decrease of the current velocity is arising. There is no separation of the current in the channels from Fig. 7. However, current velocity slightly declines behind the channels. Then, to measure exact information, the location of the base should be adjusted and the sensor on the observation window also should move forward.

The coefficient of drag C_D with and without the fines on the model experiments are shown in Fig. 8. According to the results, the drag F_D on the current velocity 0.75m/s was 0.258N. Estimation due to the numerical simulation was 0.298N. The difference of the drag F_D between the simulation and the model experiment is slight with 0.040N. Then, we evaluated that numerical analysis was succeeded. Substituting the estimated values by the simulation for equation (11), terminal speed u_∞ of the profiler was estimated as 2.52m/s. On the downwelling condition, too early terminal speed u_∞ is dangerous to break sensor and slow u_∞ also needs lots of measuring time. Then, modifying the mass in the head of profiler, we can get proper downwelling speed fitting into the requirement.

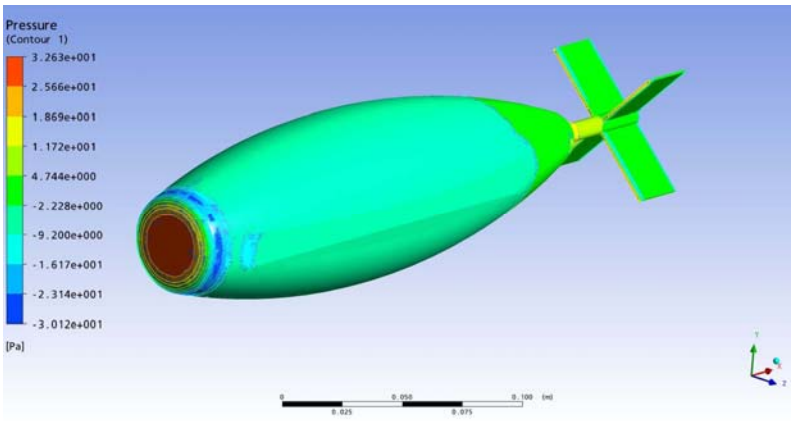

Fig. 4 Pressure distribution around the XBT profiler

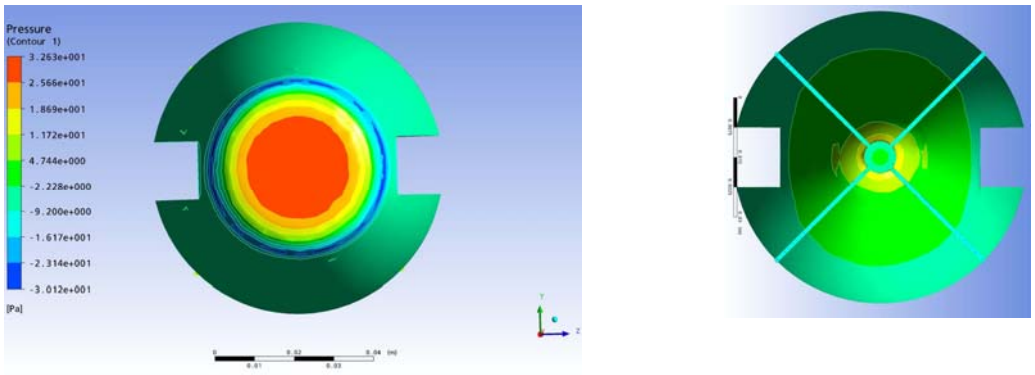

(a) front (b) back

Fig. 5 Pressure distribution around the XBT profiler

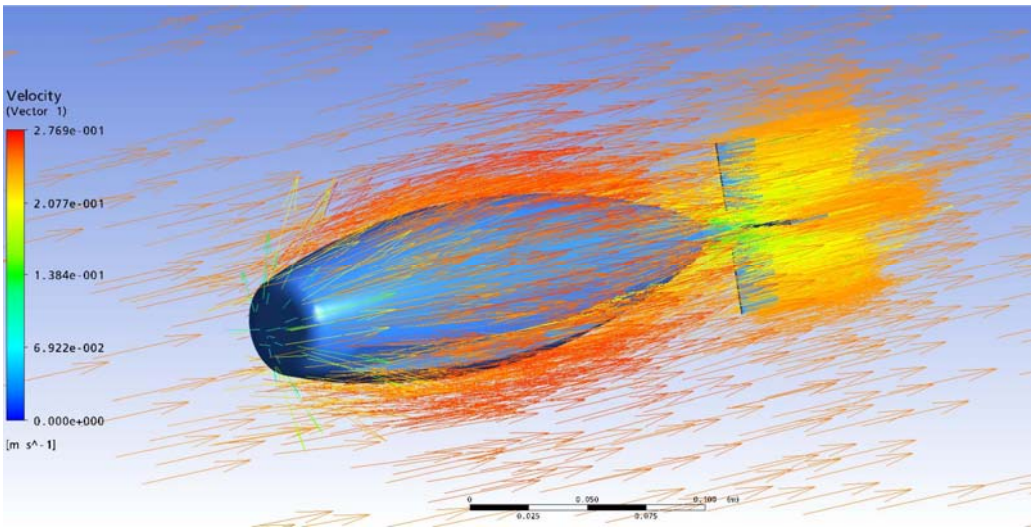

Fig. 6 Current velocity distribution around the XBT profiler

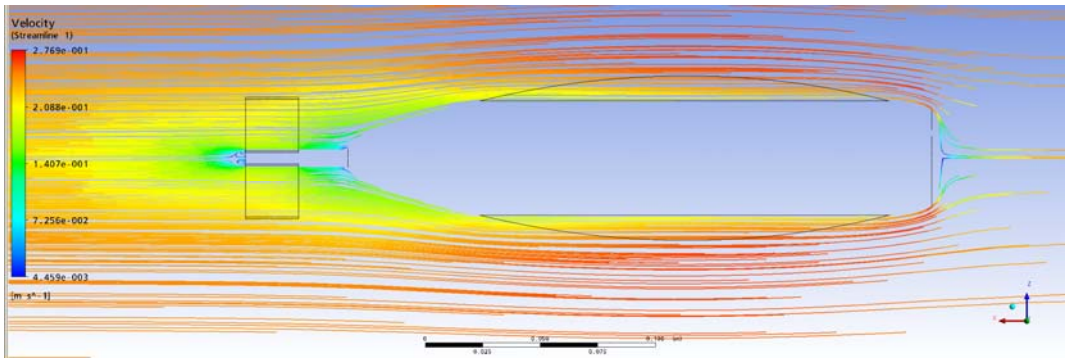

Fig. 7 Streamline around the XBT profiler

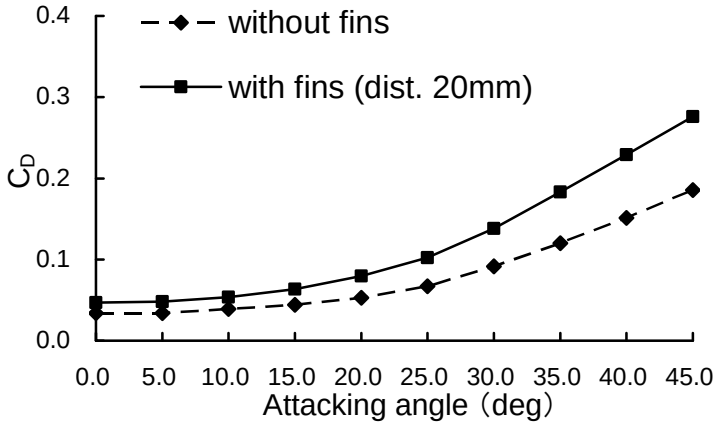

Fig. 8 C_D estimated by the model experiments

6 Conclusion

Design of a new type of XBT Profiler was significantly improved from a prototype of the frame design by using CFD technique. Not only the frame but also the proper locations of the sensor or the fines were exactly estimated based on the current velocity distribution around the profiler. Further, verification for physical value due to the simulations was conducted based on the model test used by the water tunnel. In early stage of design, we especially focused on improving the downwelling velocity due to the reduction of the drag F_D. However, reliability measured information is the most important, the required terminal speed u_∞ was reduced to approximately 2.5m/s to get stable current for the probes of sensor on the observation windows in the channels. As the results, requirements for the frame design were sufficiently achieved

and total cost for the design could be deducted.

Acknowledgements

The authors would like to sincerely thank to A. Nishimura in graduate student of Hokkaido University. The authors acknowledge the financial support from “Project of proposal-based technologic development” of the Ministry of Economy, Trade and Industry, 2007. Consequently, the result of the study led to the construction of the practical marine communication system (patent number: 4316650).

References

[1] A. Nishimura: Frame design of the new XBT profiler by the use of numerical hydrodynamic analysis, Master’s thesis, *Hokkaido University*, (2009).

[2] T. Kitano *et al*.: The analysis of the wind environment around piers with finite element method, *Mathematical and Physical Fisheries Sciences*, **6**, 89-101 (2008).

[3] ANSYS Engineering analysis, study group of CAD/CAE, *rikougakusya*, (2005).

[4] S. Komurasaki.: Simulation of a Flow around a Cylindrical Body, CFD2006, E2-3,1-4(2006).

[5] Y. Sasao et al.: 3-D simulation of unsteady turbulent flow with condensation through stream-turbine stator-rotor channels, CFD2006, B5-2,1(2006).

Received
Accepted

Academic backgrounds:

Kotarou TETSUMURA

04/1987 – 03/1991	Faculty of Fisheries, Hokkaido University, Japan
04/1991 – 03/1993	Master’s course of Graduate School of Fisheries, Hokkaido University, Japan
04/1993 –	SEC Co., Ltd, Hokkaido, Japan

Research field: Electronic engineering, Fishery mechanics, Software engineering

Nariyuki MOUNA

04/1981 – 03/1985	Faculty of Engineering, Shibaura Institute of Technology, Japan
04/1985 – 04/1989	Sawahuji, Ltd, Japan.
05/1989 –	SEC Co., Ltd, Hokkaido, Japan

Research field: Semiconductor physicality, Electronic device, Communication system

Yasuzumi Fujimori

04/1975 – 03/1980	Faculty of Fisheries, Tokyo University of Fisheries, Japan
04/1980 – 03/1981	Specialized Training Course in Pelagic Fishery, Faculty of Fisheries, Tokyo University of Fisheries, Japan
04/1982 – 03/1984	Master's course, Tokyo University of Fisheries, Japan
04/1984 – 03/1986	Doctor's course, Tokyo University of Fisheries, Japan
04/1994– 03/2005	Assistant Professor, Hokkaido University, Japan
04/2005 –	Associate Professor, Hokkaido University, Japan

Research field: Fishing technology, Gear efficiency and selectivity, Fish behaviour

Nobuo Kimura

04/1975 – 03/1980	Faculty of Fisheries, Hokkaido University, Japan
04/1980 – 03/1981	Specialized Training Course in Pelagic Fishery, Faculty of Fisheries, Hokkaido University, Japan
04/1982 – 03/1984	Master's course of Graduate School of Fisheries, Hokkaido University, Japan
04/1984 – 04/1986	Doctor's course of Graduate School of Fisheries ,Hokkaido University, Japan
05/1986 – 03/1991	Assistant Professor, Hokkaido University, Japan
04/1991 – 03/2005	Associate Professor, Hokkaido University, Japan
04/2005 –	Professor, Hokkaido University, Japan

Research field: Seakeeping quality of fishing vessel, Fishing engineering, Fluid dynamics

Appendix

1 Fundamental equation of fluid substance

Considering the law of conservation of mass, the continuity equation is derived as follow:

$$\frac{\partial \rho}{\partial t}+\frac{\partial(\rho u)}{\partial x}+\frac{\partial(\rho v)}{\partial y}+\frac{\partial(\rho w)}{\partial z}=0 \tag{1}$$

Supposed an incompressible flow of a Newtonian fluid, density ρ is constant. Then, the continuity equation is indicated as follow:

$$\frac{\partial u}{\partial x}+\frac{\partial v}{\partial y}+\frac{\partial w}{\partial z}=0 \tag{2}$$

On the law of the conservation of momentum, the motion equations of a Newtonian fluid, so-called Navier-Stokes (NS) equation, are derived by applying Newton's second law to fluid motion.

$$\begin{aligned}
\rho\frac{Du}{Dt}&=\rho\left(\frac{\partial u}{\partial t}+u\frac{\partial u}{\partial x}+v\frac{\partial u}{\partial y}+w\frac{\partial u}{\partial z}\right)=\rho F_x-\frac{\partial p}{\partial x}+\nu\left(\frac{\partial^2 u}{\partial x^2}+\frac{\partial^2 u}{\partial y^2}+\frac{\partial^2 u}{\partial z^2}\right)\\
\rho\frac{Dv}{Dt}&=\rho\left(\frac{\partial v}{\partial t}+u\frac{\partial v}{\partial x}+v\frac{\partial v}{\partial y}+w\frac{\partial v}{\partial z}\right)=\rho F_y-\frac{\partial p}{\partial y}+\nu\left(\frac{\partial^2 v}{\partial x^2}+\frac{\partial^2 v}{\partial y^2}+\frac{\partial^2 v}{\partial z^2}\right)\\
\rho\frac{Dw}{Dt}&=\rho\left(\frac{\partial w}{\partial t}+u\frac{\partial w}{\partial x}+v\frac{\partial w}{\partial y}+w\frac{\partial w}{\partial z}\right)=\rho F_z-\frac{\partial p}{\partial z}+\nu\left(\frac{\partial^2 w}{\partial x^2}+\frac{\partial^2 w}{\partial y^2}+\frac{\partial^2 w}{\partial z^2}\right)
\end{aligned} \tag{3}$$

Here, $\frac{D}{Dt}$ is the Lagrange type time derivative. F_x, F_y, F_z are the external forces and u, v, w are the flow velocities in x, y, z directions, respectively. ρ is the fluid density, p is the pressure. Standardized Navier-Stokes equations were rewritten as follows:

$$\begin{aligned}
\frac{Du}{Dt}&=\frac{\partial u}{\partial t}+u\frac{\partial u}{\partial x}+v\frac{\partial u}{\partial y}+w\frac{\partial u}{\partial z}=-\frac{1}{\rho}\frac{\partial p}{\partial x}+\nu\nabla^2 u+F_x\\
\frac{Dv}{Dt}&=\frac{\partial v}{\partial t}+u\frac{\partial v}{\partial x}+v\frac{\partial v}{\partial y}+w\frac{\partial v}{\partial z}=-\frac{1}{\rho}\frac{\partial p}{\partial y}+\nu\nabla^2 v+F_y\\
\frac{Dw}{Dt}&=\frac{\partial w}{\partial t}+u\frac{\partial w}{\partial x}+v\frac{\partial w}{\partial y}+w\frac{\partial w}{\partial z}=-\frac{1}{\rho}\frac{\partial p}{\partial z}+\nu\nabla^2 w+F_z
\end{aligned} \tag{4}$$

Here

$$\nu = \frac{\mu}{\rho} \tag{5}$$

$$\nabla^2 = \frac{\partial^2}{\partial x^2} + \frac{\partial^2}{\partial y^2} + \frac{\partial^2}{\partial z^2} \tag{6}$$

where, ν: dynamic viscosity, μ: viscous modulus and ∇^2: the laplacian. In the equations (4), the left side is called an inertia term and each term on a right side is in turn called a pressure term, a viscous term, and an external force term, respectively. Then, we can get the solution of incompressible viscous flow by solving the simultaneous equations (2), (4).

2 Formulation of the fundamental equation [3]

To simplify explanation about the formulation of the NS equations (4), we indicate the formulation related to the 2D steady flow, which is not considered for the term in the z direction.

Supposed as the permanent stream, first term on a right side in the function (4) can be ignored, and the fluid density ρ is constant because of the incompressible flow. Formulation of the fundamental equation is used by the Galerkin method that is one of weighted residual methods. The weighting functions u^*, v^* and p^* multiplied into each term of the equations (2), (4), and performed integration about the analytic area *V*. As the partial integrations are conducted for the pressure terms and viscous terms, the equations are transformed as follows:

Continuity equation:

$$\int_V p^* \left(\frac{\partial u}{\partial x} + \frac{\partial v}{\partial y} \right) dxdy \tag{7}$$

Motion equations:

$$\iint_V u^* \left(u \frac{\partial u}{\partial x} + v \frac{\partial u}{\partial y} \right) dxdy - \iint_V \left(\frac{1}{\rho} \right) \frac{\partial u^*}{\partial x} p dxdy + \nu \iint_V \left(\frac{\partial u^*}{\partial x} \frac{\partial u}{\partial x} + \frac{\partial u^*}{\partial y} \frac{\partial u}{\partial y} \right) dxdy$$
$$= -\int_C \left(\frac{n_x}{\rho} \right) u^* p ds + \nu \int_C u^* \left(n_x \frac{\partial u}{\partial x} + n_y \frac{\partial u}{\partial y} \right) p ds$$

$$\iint_V v^*\left(u\frac{\partial v}{\partial x}+v\frac{\partial v}{\partial y}\right)dxdy-\iint_V\left(\frac{1}{\rho}\right)\frac{\partial v^*}{\partial x}pdxdy+\nu\iint_V\left(\frac{\partial v^*}{\partial x}\frac{\partial v}{\partial x}+\frac{\partial v^*}{\partial y}\frac{\partial v}{\partial y}\right)dxdy$$
$$=-\int_C\left(\frac{n_y}{\rho}\right)v^*pds+\nu\int_C v^*\left(n_x\frac{\partial v}{\partial x}+n_y\frac{\partial v}{\partial y}\right)pds \tag{8}$$

Here, suffix C indicates the whole boundary of the analytic area V, and n_x and n_y indicate the direction cosine in the x and y directions of the normal line n on the C, respectively. Then, the analytic area V divides into the elements and the interpolations are done in each element by the use of the form function ϕ_e of u, v, and p.

$$\begin{aligned} u &= \phi_e u_{ie}, \\ v &= \phi_e v_{ie}, \\ p &= \phi_e p_{ie} \quad (i=1,2,3,4) \end{aligned} \tag{9}$$

Here, u_{ie}, v_{ie} and p_{ie} are the values of u, v and p at the node of the element, respectively. As the Galerkin method with the weighting functions u^*, v^* and p^* as the complementary function, the functions are expressed as follows:

$$\begin{aligned} u^* &= \phi_e u^*_{ie}, \\ v^* &= \phi_e v^*_{ie}, \\ p^* &= \phi_e p^*_{ie} \quad (i=1,2,3,4) \end{aligned} \tag{10}$$

Related to element e shown in Fig. 9, the form function $u^*_e(x)$ can be indicated as follow:

$$u^*_e(x)=\alpha_{1e}+\alpha_{2e}x+\alpha_{3e}y+\alpha_{4e}xy \tag{11}$$

Here, all from α_{1e} to α_{4e} are undetermined coefficients. Supposed that the equation (11) form in both ends' node of the element, the tangency condition related to the element e can be obtained as follow:

$$u_{ie}(x)=\alpha_{1e}+\alpha_{2e}x_{ie}+\alpha_{3e}y_{ie}+\alpha_{4e}x_{ie}y_{ie} \tag{12}$$

Here, node number $i=1_e,2_e,3_e,4_e$. From the equations (11) and (12), $u^*_e(x)$ is indicated by the linear expression from u_{1e}, to u_{4e}. Then, supposed that the basis function $\phi_{ie}(x,y)$ is defined in the each element, $u^*_e(x)$ can be indicated as follow:

$$u_e^*(x) = \phi_{1e}(x,y)u_{1e} + \phi_{2e}(x,y)u_{2e} + \phi_{3e}(x,y)u_{3e} + \phi_{4e}(x,y)u_{4e}$$
$$= \boldsymbol{\phi_e}(\boldsymbol{x},\boldsymbol{y})\boldsymbol{u_e} \tag{13}$$

Here, $\boldsymbol{\phi_e}(\boldsymbol{x},\boldsymbol{y}) = [\phi_{1e}, \phi_{2e}, \phi_{3e}, \phi_{4e}]$, $\boldsymbol{u_e}^T = = [u_{1e}, u_{2e}, u_{3e}, u_{4e}]$, and $\boldsymbol{T}$ indicates the transposed matrix.

Assuming that the velocity was fed off on the whole boundary, the right terms in the equations (8) including the line integral become zero. Further, the integration was conducted on the each element, and organized for u_{ie}^*, v_{ie}^*, and p_{ie}^*, multidimensional simultaneous equations related to u_{ie}, v_{ie} and p_{ie} are obtained as follows:

$$\begin{aligned} &H_{ijk}^x u_{le} + H_{ijk}^y v_{le} = 0 \\ &K_{ijk}^x u_{je} u_{ke} + K_{ijk}^y v_{je} u_{ke} + H_{ik}^x p_{ke} + D_{ij}^{xy} u_{je} = 0 \\ &K_{ijk}^x u_{je} v_{ke} + K_{ijk}^y v_{je} v_{ke} + H_{ik}^y p_{ke} + D_{ij}^{xy} v_{je} = 0 \end{aligned} \tag{14}$$

Here, each term in the equations (14) is expressed as follows:

$$\begin{aligned} H_{ik}^x &= -\left(\frac{1}{\rho}\right)\iint \frac{\partial \phi_{ie}}{\partial x}\phi_{ke}\,dxdy \\ H_{ik}^y &= -\left(\frac{1}{\rho}\right)\iint \frac{\partial \phi_{ie}}{\partial y}\phi_{ke}\,dxdy \\ K_{ijk}^x &= \iint \phi_{ie}\phi_{je}\frac{\partial \phi_{ke}}{\partial x}\,dxdy \\ K_{ijk}^y &= \iint \phi_{ie}\phi_{je}\frac{\partial \phi_{ke}}{\partial y}\,dxdy \\ D_{ij}^{xy} &= \nu\iint\left(\frac{\partial \phi_{ie}}{\partial x}\frac{\partial \phi_{je}}{\partial x} + \frac{\partial \phi_{ie}}{\partial y}\frac{\partial \phi_{je}}{\partial y}\right)dxdy \end{aligned} \tag{15}$$

Superposed the element matrix in the whole elements, all of the equations are shown in following matrix.

$$\begin{bmatrix} 0 & \sum_e \boldsymbol{H}_{ik}^{xT} & \sum_e \boldsymbol{H}_{ik}^{yT} \\ \sum_e \boldsymbol{H}_{ik}^{x} \boldsymbol{p}_k & \sum_e (\boldsymbol{K}_{ijk}^{x} \boldsymbol{u}_j + \boldsymbol{K}_{ijk}^{y} \boldsymbol{v}_j + \boldsymbol{D}_{ij}^{xy}) & 0 \\ \sum_e \boldsymbol{H}_{ik}^{y} \boldsymbol{p}_k & 0 & \sum_e (\boldsymbol{K}_{ijk}^{x} \boldsymbol{u}_j + \boldsymbol{K}_{ijk}^{y} \boldsymbol{v}_j + \boldsymbol{D}_{ij}^{xy}) \end{bmatrix} \begin{bmatrix} \boldsymbol{p} \\ \boldsymbol{u} \\ \boldsymbol{v} \end{bmatrix} = \begin{bmatrix} \boldsymbol{R}_1 \\ \boldsymbol{R}_2 \\ \boldsymbol{R}_3 \end{bmatrix} \tag{16}$$

Here, $\boldsymbol{R}_1, \boldsymbol{R}_2, \boldsymbol{R}_3$ are residuals. The equations (16) are nonlinear equations which the coefficient matrices are expressed as the function related to the unknown $\boldsymbol{u}$ and $\boldsymbol{v}$.

The formulation in the case of the 3D steady flow can conduct by the abovementioned procedure by considered the z direction in the equations (2) and (4).

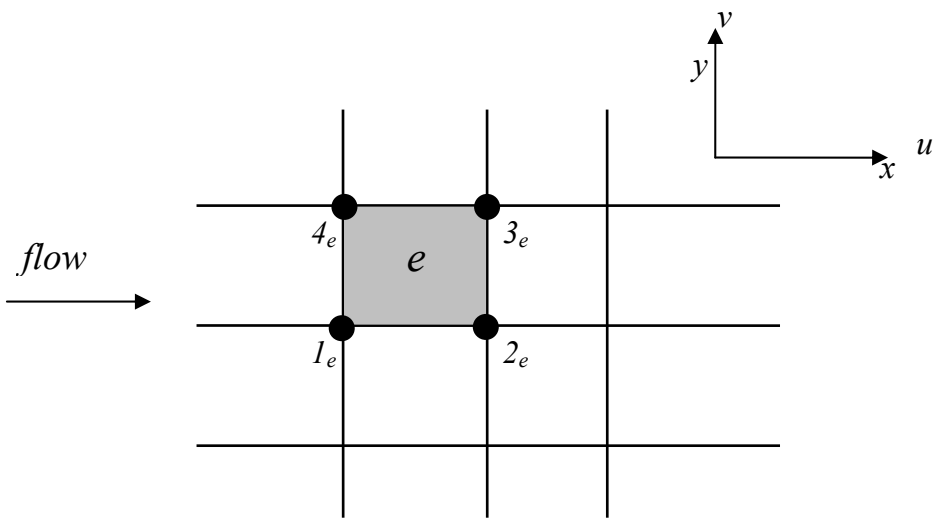

Fig. 9 Quadrilateral element with four nodes

3 Motion equation

Focusing on the downwelling velocity of the profiler, 1st dimensional motion equation in the vertical direction is expressed as follow:

$$(m + m_x)\frac{du}{dt} = mg - V\rho - F_D \tag{17}$$

where, m: mass, m_x: added mass in the vertical direction, V: volume, F_D: drag, g: gravity acceleration.

As the drag F_D is generally proportional to the square of the speed u^2, the equation (17) is expressed as follow:

$$\left(m+m_x\right)\frac{du}{dt}=mg-V\rho-\frac{1}{2}C_D\rho Au^2 \tag{18}$$

where, C_D: coefficient of drag, A: projected area.

As the equation (18) is separable, we separate variable and integrate as follow:

$$\int tdt=\int\frac{m+m_x}{mg-V\rho-\frac{1}{2}C_D\rho Au^2}du \tag{19}$$

Solving for u, we can get the next equation.

$$u=\sqrt{\frac{mg-V\rho}{\frac{1}{2}C_D\rho A}}\tanh\left(\frac{\sqrt{\frac{1}{2}C_D\rho A}\cdot\sqrt{mg-V\rho}}{m+m_x}t\right) \tag{20}$$

As $t\to\infty$, the term of tanh converges into 1, then we can estimate the terminal velocity u_∞ as follow:

$$u_\infty\cong\sqrt{\frac{mg-V\rho}{\frac{1}{2}C_D\rho A}} \tag{21}$$